FAULT CHARACTERISATION AND CLASSIFICATION USING WAVELET AND FAST FOURIER TRANSFORMS

E. E NGU, K. RAMAR
Multimedia University
FOE, MMU, Persiaran Multimedia, 63100
MALAYSIA
eengu@mmu.edu.my, ramar@mmu.edu.my

R. MONTANO, V. COORAY
High Voltage Valley
Fredsgatan 27, P.O.Box 832, SE-77128 Ludvika
SWEDEN
raul.montano@highvoltagevalley.org,
Vernon.Cooray@angstrom.uu.se

Abstract: - In order to improve the power quality maintenance and reliability of power supply, different types of faults on the transmission line namely: open-circuit (OC), short-circuit (SC), high impedance faults (HIF) and the fault caused by direct lightning strike (LS) have been investigated in this paper. The disturbances have been modelled and simulated using a well-known transient simulation tool - Alternative Transient Program/ Electromagnetic Transient Program (ATP/EMTP) and the resulting data are then imported into MATLAB for the investigation on the traveling wave (TW) reflection pattern and harmonic behaviour . Study on the characteristics of the faults in terms of their corresponding frequency spectrum, the polarities of the incident-wave and reflected-wave has been performed and the possibility to differentiate the type of fault is explored. For this purpose, the fault on the wave has been created at the moment when the voltage signal reaches its peak and also when it is close to zero. Both, Wavelet Transform (WT) and Fast Fourier Transform (FFT) methods have been used to analyze the transient signals generated by the fault. Model of the network used in this study is taken from [1]-[2].

Key-words: - WT, FFT, ATP/EMTP, current reflection pattern, and spectrum analysis

1 INTRODUCTION

With the continuous and rapid extension of power networks, development of automatic and reliable technique for fault detection and location has recently received considerable attention. It is well-known that high frequency transient signals will be generated whenever disturbances occur, where the power network will lose its steady state condition, resulting in a large number of cases with load drops. Thus, a robust and stable fault location technique is required not only for fast fault clearance to restore electricity supply, but also the safety of power networks and human life.

During the past decade different kinds of fault location algorithms either based on the single- or double-end synchronized and unsynchronized measurement methods, associated with different kinds of analysis techniques such as WT, neural network, travelling wave (TW), etc. have been developed. However, studies associated with the characterization of the types of disturbances/fault in relation to the various methodologies/ techniques used for fault detection has not been extensively reported in the literature.

Power quality monitoring under different types of faults is very important in electrical power generation, transmission and distribution. Therefore, the detection and classification of type of disturbance must not be neglected.

In this paper, a brief introduction to WT and FFT is given in Section 2. Section 3 describes a method to obtain high frequency transient signals by simulating a Power System using ATP/EMTP for various types of faults. Study on the characteristic of SC, OC, HIF and LS types of faults based on their frequency content and the polarity of incident and reflected waves from the fault point as well as from the neighboring and/or remote end busbars is given in Section 4. For this study the MATLAB Wavelet Toolbox has been used. Section 5 gives the discussion and conclusion.

2 REVIEW OF TRAVELLING WAVE (TW) THEORY AND TRANSFORM TECHNIQUES

2.1 Travelling Wave Theory

According to TW theory, any disturbance or a sudden change in an overhead transmission line or underground cable will generate both forward and backward TWs signals propagating away from the disturbance point towards both busbars. The initial values of these waves are dependent on several factors such as fault position, fault path resistance, fault inception angle [3], type of fault, etc. Further, these signals will be reflected and refracted at the points of discontinuity, i.e., fault point and busbars, until they are attenuated to a negligible value. The basic principle of this method can be well explained using Bewley lattice diagram as illustrated in Fig. 1.

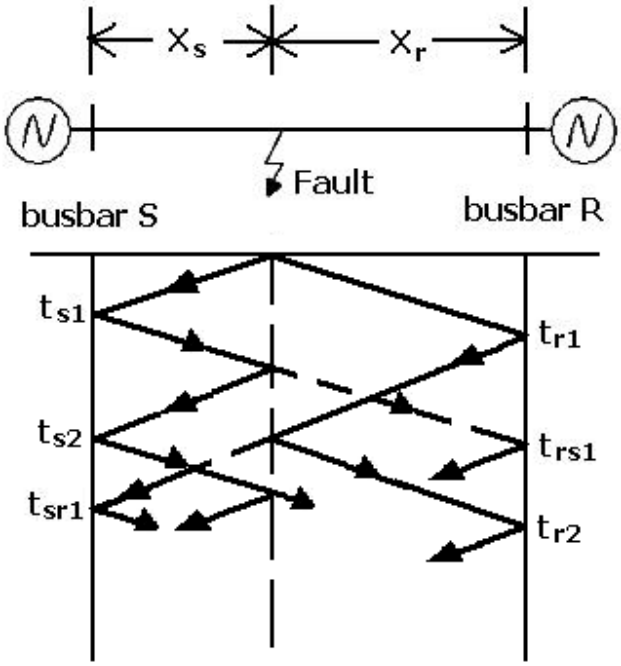

Fig. 1: Bewley lattice diagram.

The generated transient signals consisting of different high frequency components with information on the type of fault can be used to locate the fault. Since the main objective in this investigation is to classify the type of fault based on the polarity of reflected waves from the point of discontinuity, details on the methodology used to identify/estimate the fault location are not discussed. Furthermore, the basic fault location and calculation method based on the TW has been well documented in the literature [4]-[7].

Based on the measurements taken at both busbars, S and R (see Fig. 1), the fault distance (x_s) and (x_r) can be calculated using equation (1) and (2) respectively as:

$$x_s = \frac{t_{s2} - t_{s1}}{2} v \quad (1)$$

$$x_r = \frac{t_{r2} - t_{r1}}{2} v \quad (2)$$

where t_{s1} and t_{r1} are times for incident waves to reach busbar S and R respectively, t_{s2} and t_{r2} are the moment the reflected wave from fault point arrive at busbar S and R respectively, t_{sr1} and t_{rs1} are arrival time for the wave reflected from remote end busbars, L is the total length of the line and v is the wave propagation speed.

2.2 Wavelet and Fast Fourier Transforms

One of the interesting similarities between Wavelet Transform (WT) and Fourier Transform (FT) is that their basic functions are localized in the frequency domain; providing the users useful information on the operating conditions of the power distribution network. Since the transient signals generated by disturbances are non-stationary signals associated with a wide range of frequencies superimposed to the power frequency component, it is not advisable to apply a methodology associated with FT as the analysis tool.

FT has various constraints and limitations associated with time-frequency resolution where it is not possible to identify at what times these high frequency components occurred, these limitations are not present in WT methodology. Time information is very important in locating the fault position and thus WT always become more applicable/ useful while analyzing non-stationary signals. Moreover, WT provides the capability to localize the transient signal in time- and frequency-domain.

The difference between WT and FT can be well explained using Fig. 2. It can be seen from Fig. 2(a) that FT is using a single fixed size squared window in the whole transformation process and thus there will be no difference on the resolution. On the other hand, WT is using a windowing technique with variable-sized region on the time-frequency plane as shown in Fig. 2(b). Therefore, it has the capability to analyse a given signal with different resolutions at different frequencies.

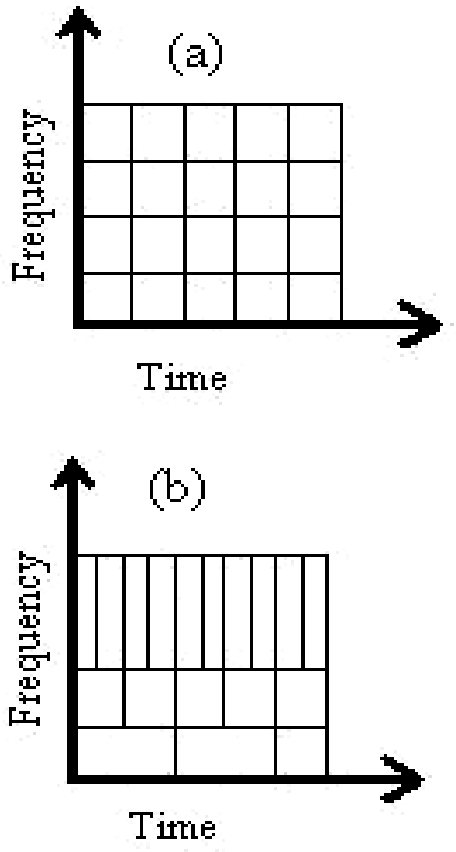

Fig. 2: Coverage on time-frequency plane by (a) FT, and (b) WT basic functions.

However, if one is interested to know what the frequency content of a signal is; FT will a more suitable alternative. Detailed theory of wavelet analysis and comparison with Fourier analysis can be found in [8]-[11].

3 SIMULATION STUDY CASES

3.1 APT/EMTP Power System Modeling

A simple two-end power system model (Fig. 3) with some of the system parameters and transmission line configuration (Fig. 4) being adapted from [1] and [2] respectively, has been used to study the characteristics of SC, OC, HIF and LS.

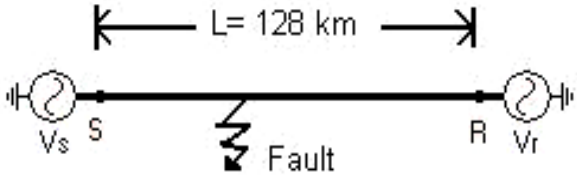

Fig. 3: Typical 400-kV three-phase overhead transmission line [1].

I<SKE>	<ACRESI>	IX<	REAC ><	DIAM ><	HORI ><	VTOWER><	VMID ><	SEPAR ><	ALPH>	NB
0	0.0	0.0663	3	0.7788	2.959	2.90	37.60	37.60		1
0	0.0	0.0663	3	0.7788	2.959	18.30	37.60	37.60		1
1	0.0	0.0663	3	0.7788	2.959	0	26.6362	26.6362		1
1	0.0	0.0663	3	0.7788	2.959	-0.2285	27.0319	27.0319		1
1	0.0	0.0663	3	0.7788	2.959	0.2285	27.0319	27.0319		1
2	0.0	0.0663	3	0.7788	2.959	10.60	32.0362	32.0362		1
2	0.0	0.0663	3	0.7788	2.959	10.3715	32.4319	32.4319		1
2	0.0	0.0663	3	0.7788	2.959	10.8285	32.4319	32.4319		1
3	0.0	0.0663	3	0.7788	2.959	21.20	26.6362	26.6362		1
3	0.0	0.0663	3	0.7788	2.959	20.9715	27.0319	27.0319		1
3	0.0	0.0663	3	0.7788	2.959	21.4285	27.0319	27.0319		1

Fig. 4: Tower configuration used in the study generated using manual bundling in ATP Line Constants supporting program [2].

The test system with the transposed and distributed Clarke transmission line of 128 km and a three-phase short circuit levels of 5GVA and 35 GVA at busbars S and R respectively has been simulated using ATP/EMTP with 50 Hz power frequency, assuming perfect conducting ground condition.

In our previous preliminary study reported in [1], a balance network was modelled and studied using ATPDraw. But in practice the network may not be balanced. In this paper the study done in [1] for balanced network is repeated with the following parameters:

$$Z_{s0}/Z_{s1} = Z_{r0}/Z_{r1} = 0.5$$
$$Z_{s1} = (33.255 + j4.434)\ \Omega$$
$$Z_{r1} = (4.751 + j6.334)\ \Omega$$

with Z_{s0} and Z_{s1} is zero and positive surge impedance at busbar S respectively, Z_{r0} and Z_{r1} is zero and positive surge impedance at busbar R respectively.Workflow of the simulation and analysis has been summarized in Fig. 5.

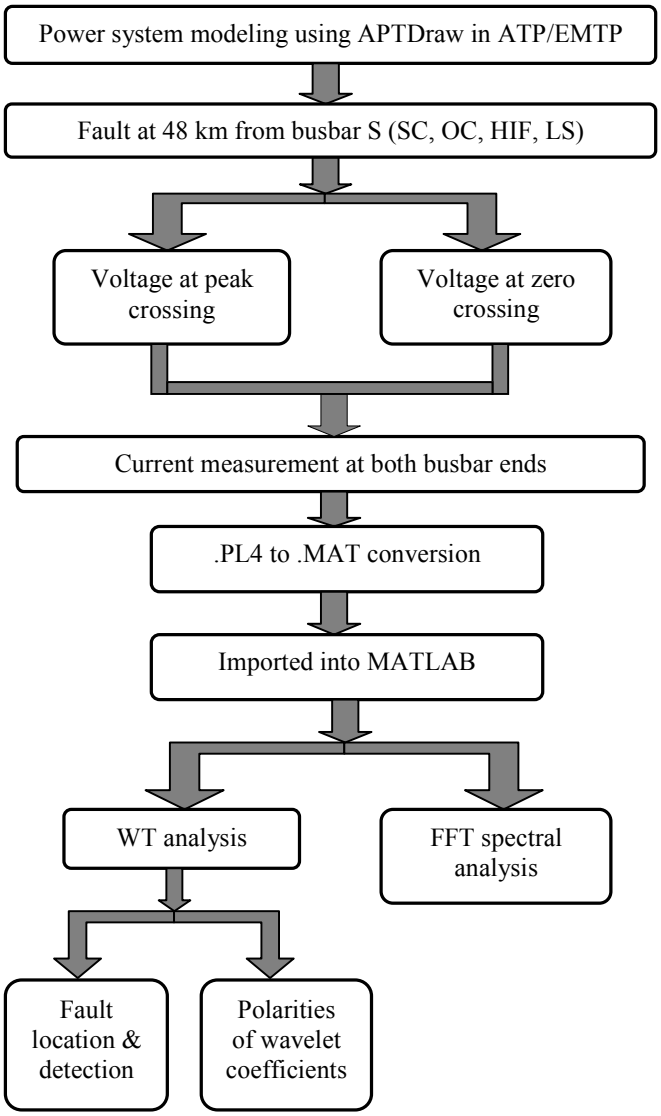

Fig. 5: Flowchart

3.2 Study Cases

A small fault resistance of 0.1 milli-ohm has been used in the study of the SC fault between phase A and ground (A-G) while for the HIF the fault the model proposed in [12] has been chosen. In the lightning surge study, a short pulse of 10 kA, 8/20 μs has been injected to phase A for shielding failure study [8]. Similarly the fault has been created at phase A for OC test.

To study the signal reflection pattern, the calculated current signals have been taken at both ends, so that the reflection polarities at these ends can be identified to give the whole picture on the characteristic of different types of faults. However, only the estimated sending current will be used in fault distance calculation. For the sake of comparison, the faults have been created at the point when the voltage wave is close to its peak, V_p (hereafter called V_p-fault) and at zero crossing, V_0 (hereafter called V_0-fault). The sampling rate of 1 MHz has been chosen in this study. The faults have been created at 48 km from busbar S.

4 FAULT DETECTION, LOCATION AND CLASSIFICATION

Figure 6(a) shows the voltage and current waveforms when the SC fault occurs close to the peak of the voltage wave and 6(b) shows the waveforms for SC fault close to zero voltage. Similar results have been obtained for other fault cases also.

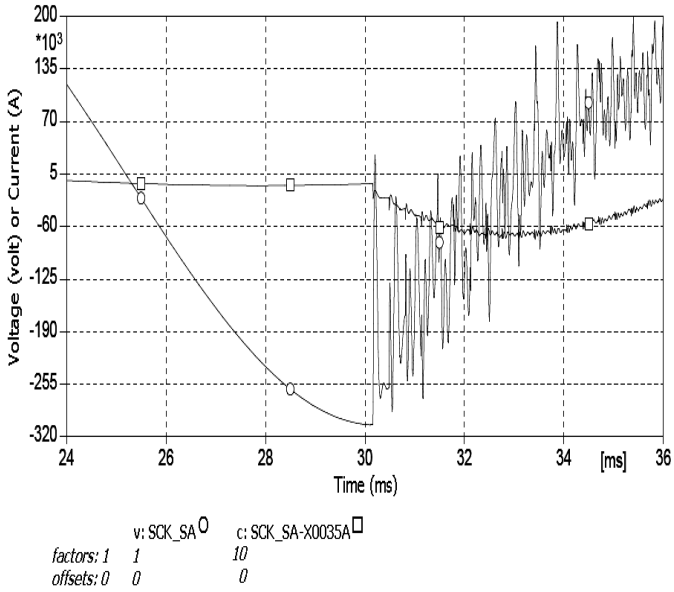

Fig. 6(a): Voltage and current waveforms for fault close to the peak voltage (—o— represents voltage and —□— represents current wave).

4.1 Fault Detection and Location – Wavelet Transform

Wavelet analysis is adopted for fault detection and equations (1) and (2) are applied to obtain the location of fault on the line from busbars S and R respectively. Since WT has quite a number of mother wavelets, such as Symlets (sym), Daubechies (db), Coiflets (coif), etc., choosing a right mother wavelet is crucial in determining the resolution of time and frequency localization.

Consequently, a comparison among the sym, db and coif wavelet families has been done and the results show nominal differences among them.

As stated in [8], db wavelet families have been chosen in most studies as they are well suited to power quality analysis. Thus, db3 with level 1 (d1) coefficient has been selected to detect the singularity in the transient signals generated by the disturbances. It is to bear in mind that, level 1 carries the most information compared to levels 2, 3, etc. Higher the level, more information is lost as the frequency component will be halved from level to level. However, level 3 or 4 shall be chosen if the noise content is considerable high in level 1.

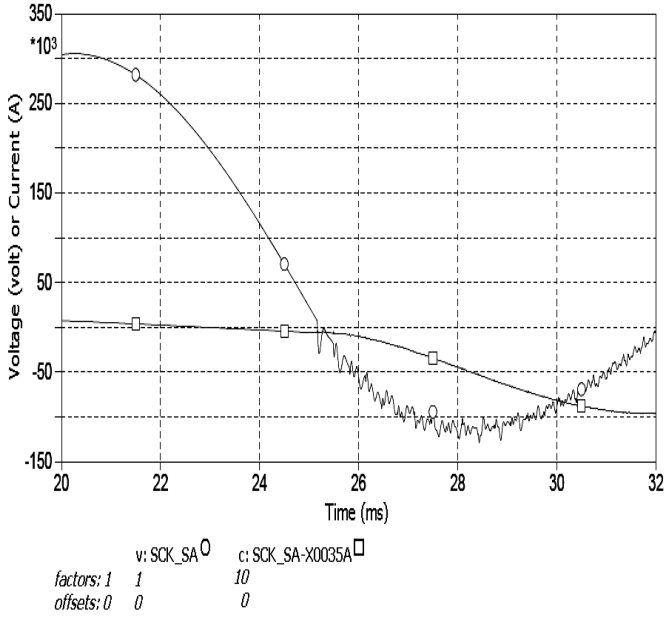

Fig. 6(b): Voltage and current waveform for fault close to zero voltage (⊸ represents voltage and ⊣⊢ represents current wave).

Figures 7 to 11 show the outputs of WT and FFT applied to the disturbed waveforms for different faults. Each figure consists of three parts. Parts (i) and (ii) show the detail of level 1 coefficients of WT applied to current signals measured at ends S and R respectively and are meant for fault detection and location. While part (iii) is the discrete plot of frequency spectrum obtained using FFT on the measured current signals that will be used in fault characterisation. For a complete understanding/ analysis, the WT coefficients shown in parts (i)-(ii) of Figs 7 to 10, have been scaled up to give a good view on the changes of the resulting coefficients.

Table 1 shows the fault position calculated using equation (1) based on the information extracted using db3, where the arrival time of the TW at the busbar is illustrated by the sudden change of the coefficients. The fault has been created at 25 ms and 30 ms for the fault close to zero voltage value, and the fault close to peak voltage value, respectively. It can be seen from Table 1 that the error in the calculated fault distance for all types of faults is within 400 m for both study cases.

Table 1
Calculated fault distance from busbar S and the percentage of the error for V_0- and V_p-faults

Type of fault		Calculated fault distance from end S, x_s (km)		Error (%)
V_0-fault	SC	Δt = 1 μs	47.67	0.68
		Δt = 100 ns	47.85	0.31
	OC	47.69		0.64
	HIF	47.97		0.06
	LS	47.68		0.68
V_p-fault	SC	Δt = 1 μs	47.66	0.70
		Δt = 100 ns	47.85	0.31
	OC	47.68		0.68
	HIF	47.68		0.68
	LS	47.65		0.74

It is worth mentioning that in SC case, simulation has been repeated with sampling time, Δt =100 ns for V_0 and V_p faults and the results are shown in Fig. 7(c). This repetition has been done as there were some inaccuracy in the polarity of the WT coefficients when the simulation is done with Δt =1μs. But there was no problem in fault location as it is decided by the appearance of the disturbance and the polarity of WT coefficients. However it is observed that the accuracy of fault location is improved with increase in sampling rate.

For fault detection and location in LS case, result obtained from the WT analysis shows that the injection of the pulse introduces only a very fast transient on the transmission line and no fault persisting on the line. Even so, the point of disturbance can still be detected and located using the information in the current signals using WT. From Table 1 it can be concluded that the fault location using WT is quite satisfactory for all types of faults.

4.2 Traveling Wave Reflection Pattern and Fault Classification – Fast Fourier and Wavelet Transforms

In this section the type of fault and its characteristic are investigated and classified using lattice diagram and spectral analysis.

It can be seen from parts (i) and (ii) of Figs 7(a) and (b) that, in the case of SC, the current wave is inverted at both the fault point and busbars and thus the reflected wave from the fault point has the same polarity as the initial wave while the one reflected from the remote end might be in opposite to or the same polarity as the initial wave [3], depending on the polarity of the initial wave at the other busbar end.

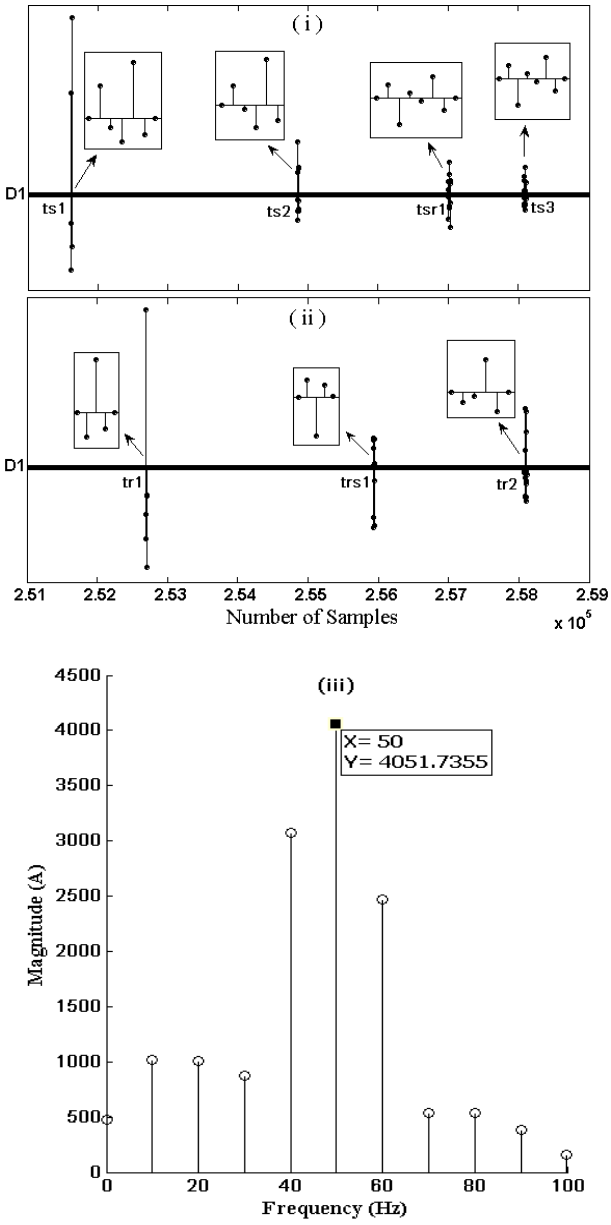

Fig. 7(a): SC fault – V_0 case.

The fundamental harmonic amplitude in this case is the highest compared to others, with the amplitude of about 4051 A and 4512 A for V_0 and V_p cases respectively.

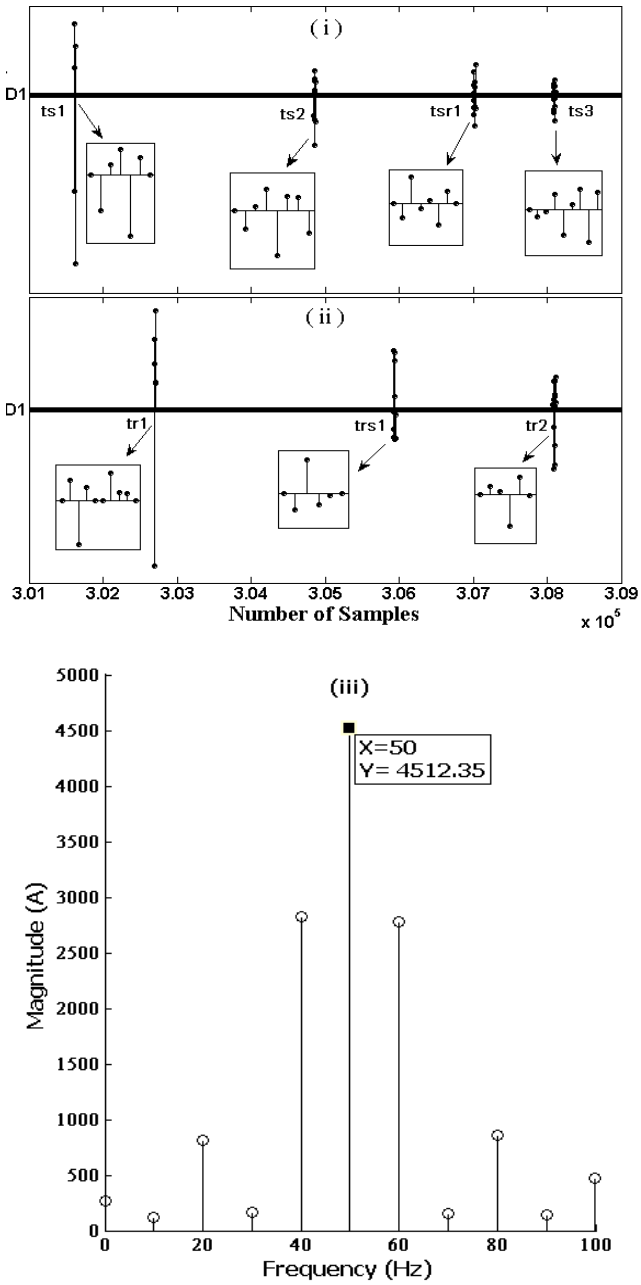

Fig. 7(b): SC fault – V_p case.

As mentioned in section 4.1 there was a problem with numerical solution in the case of SC faults, particularly in V_p case (refer to Fig. 7(c)). Thus, the simulations for

SC cases have been repeated with a smaller sampling time of 100 ns.

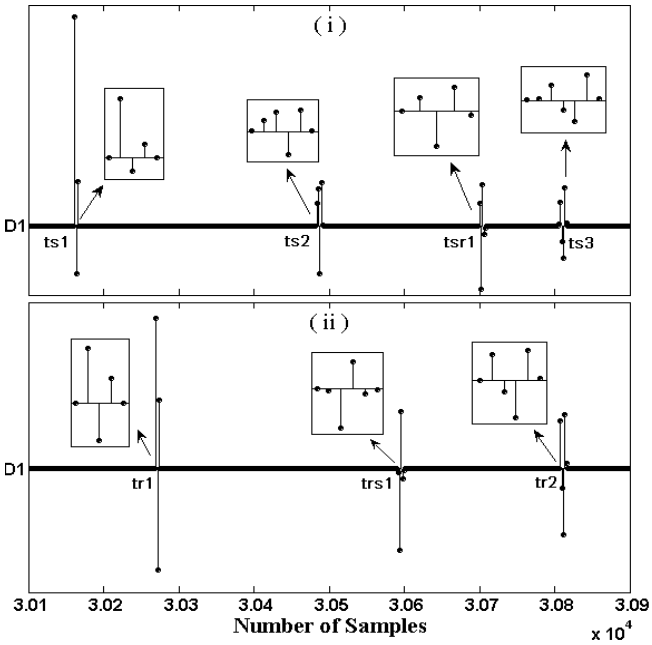

Fig. 7(c): Numerical solution problem in SC fault – V_p case with 1 μs Δt.

For the OC fault, the characteristics of the reflected wave at busbars and the fault location are such that the current signal is inverted at the busbar only but doubled at the fault point.

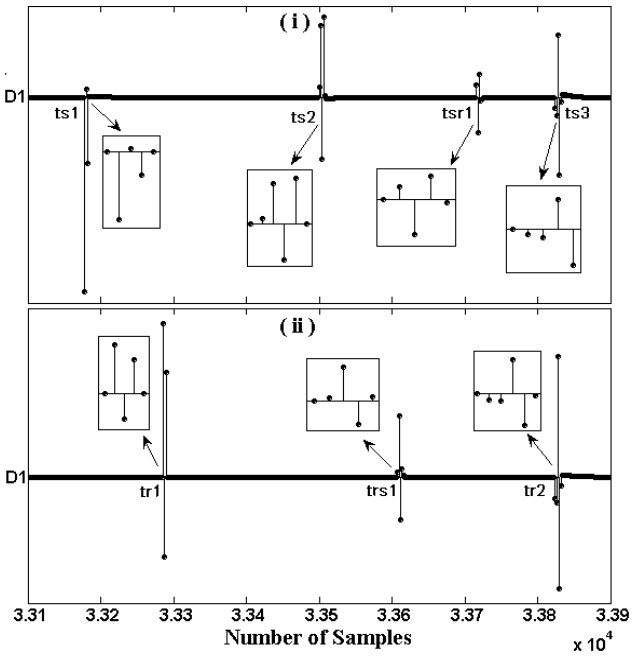

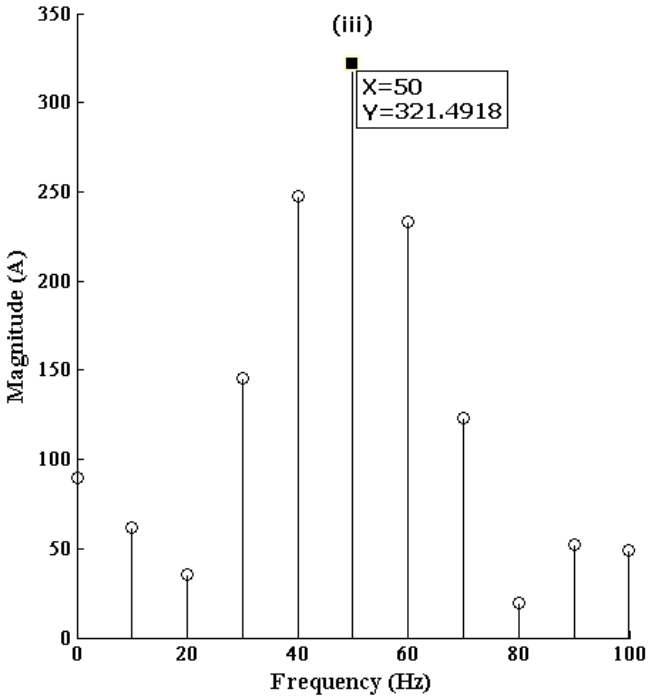

Fig. 8(a): OC fault – V_0 case.

It has been observed that this kind of fault has the smallest fundamental harmonic amplitude, which is about 321 A for both study cases, due to the fact that the circuit breaker opening time for both V_0, and V_p faults is about the same – 0.033 s.

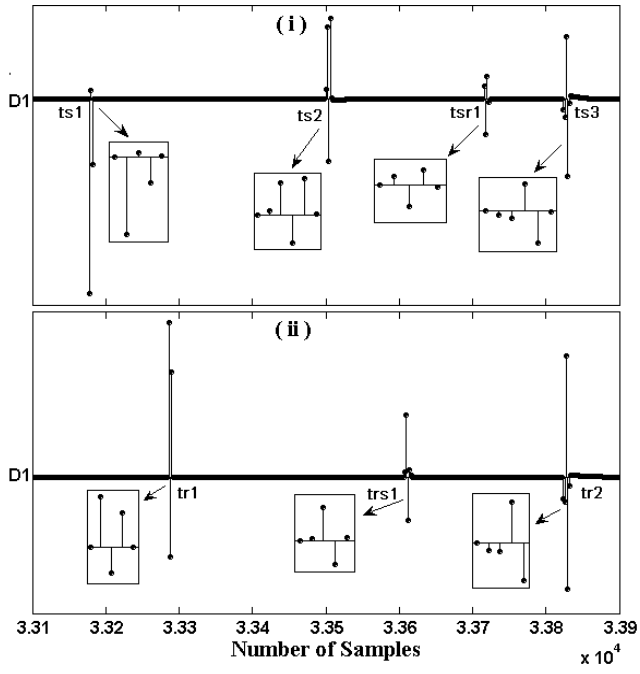

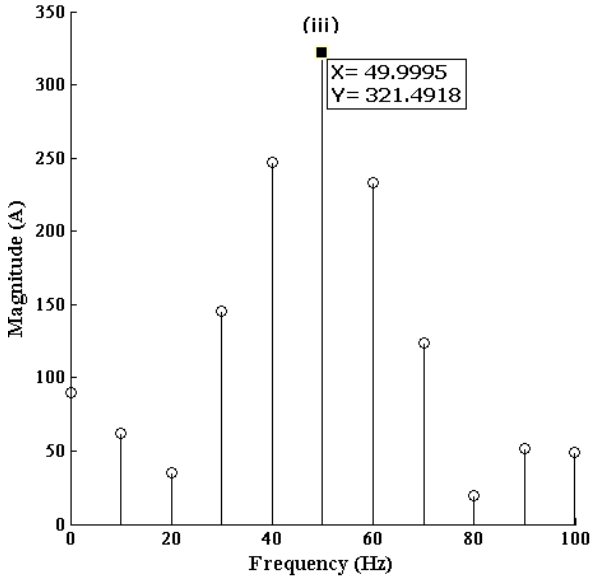

Fig. 8(b): OC fault – V_p case.

Nevertheless, as illustrated by Fig. 8(c) the amplitude of the first harmonic could reach about 410 A if the fault point-on-wave occurs at negative going transition either at the time of 0.035 s or 0.04 s. It is because for OC case, circuit breaker opening and closing time is somehow governed by magnitude of the current on the wave. It is also to bear in mind that the current resulted at the sending and receiving ends are due to the capacitive- and inductive-effect associated with the long transmission line used for the present study.

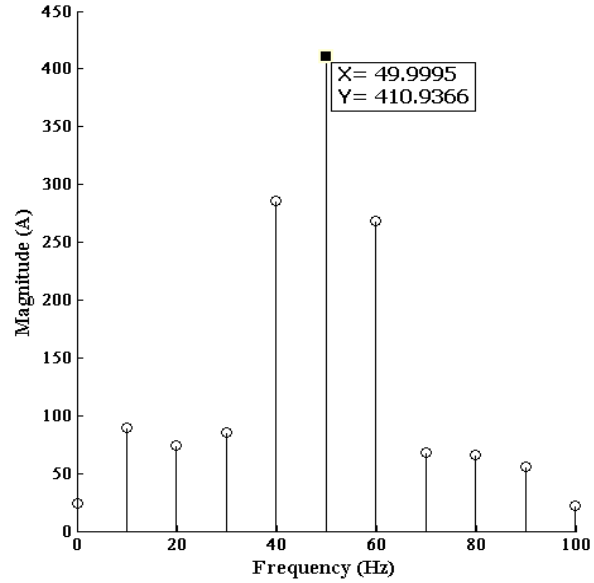

Fig. 8(c): OC fault – V_0 (0.035 s) and V_p (0.04 s) cases

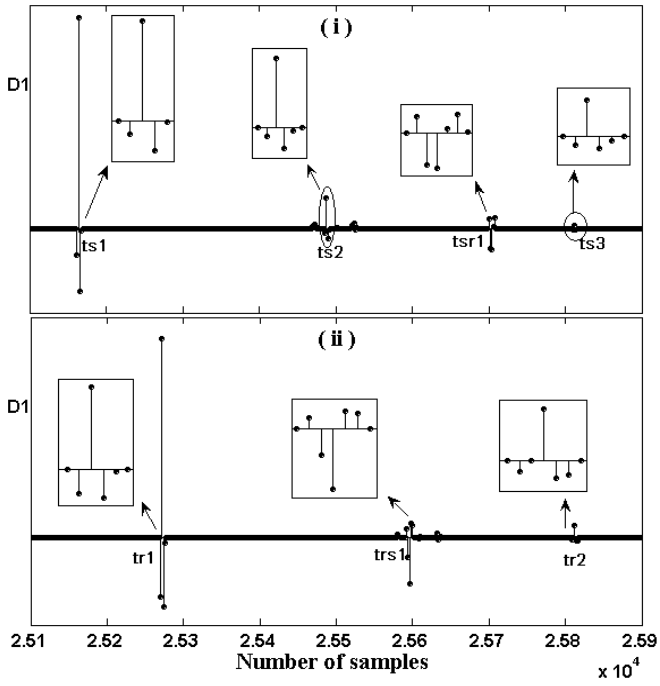

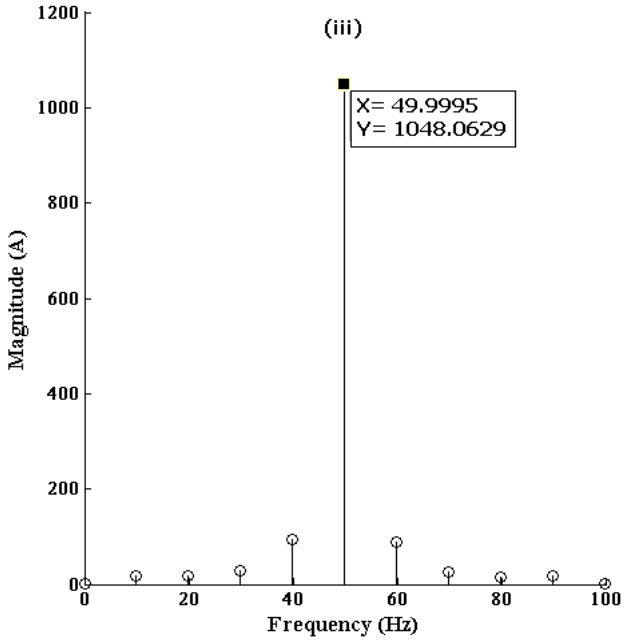

Fig. 9(a): HIF – V_0 case.

In the previous preliminary investigation on the HIF, reported in [1] it was found that characteristic of the TW reaching at busbars under V_0 condition is the same as the SC case. But, in the case of V_p, it was found that the signal was inverted at busbar R and fault point seen from R, and it was doubled at busbar S and the fault point seen from S [1]. However, in the present study with

unbalanced network it is observed that the behaviour of the HIF current TW is the same as that in SC case, where it is inverted at both fault point and busbars (as shown in Figs 9(a)-(b)) with amplitude of the first harmonics in the range of 1000 A and 1500 A.

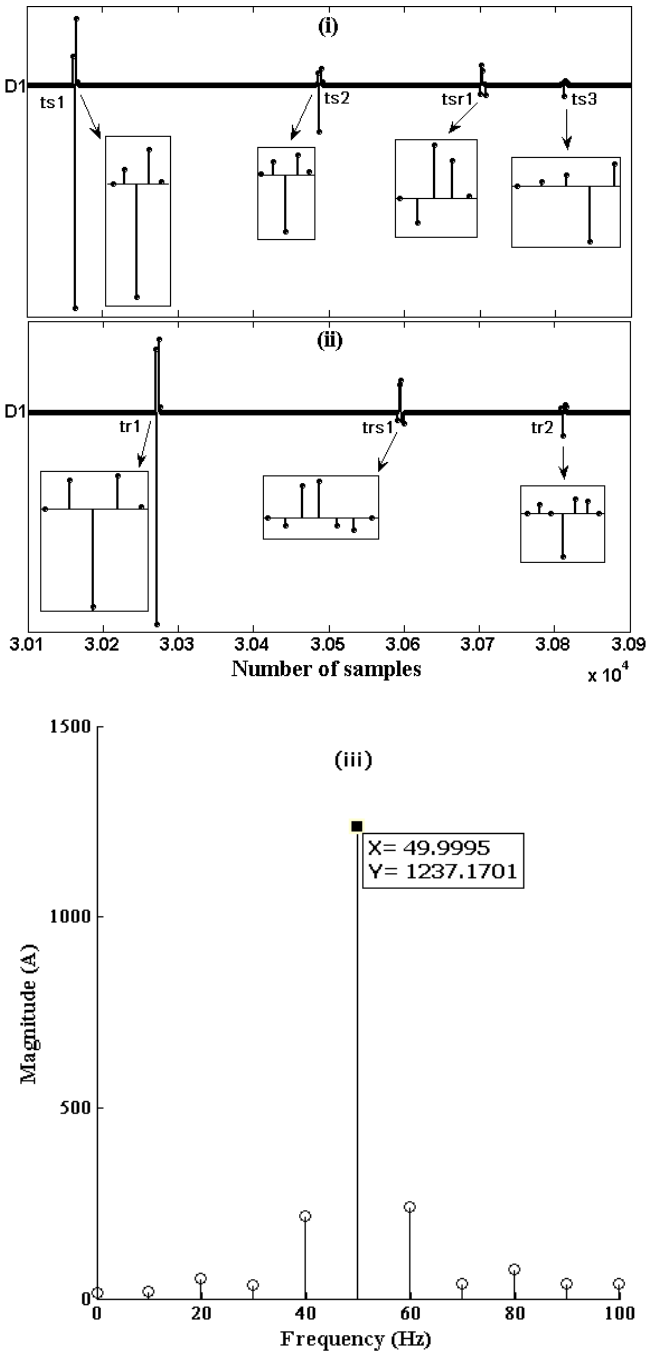

Fig. 9(b): HIF – V_p case.

Under LS fault condition, the study shows that there is no reflection occurred at the fault point after t_{s1} and t_{r1} because the fault is not persisting. But the observed second sudden changes *(t_{sr1}* and *t_{rs1})* are the ones resulted from the reflection at the remote ends, while *t_{srs1} and t_{rsr1}* are the arrival time of the initial current TWs reflected from busbars R and S respectively (as shown in Fig. 11).

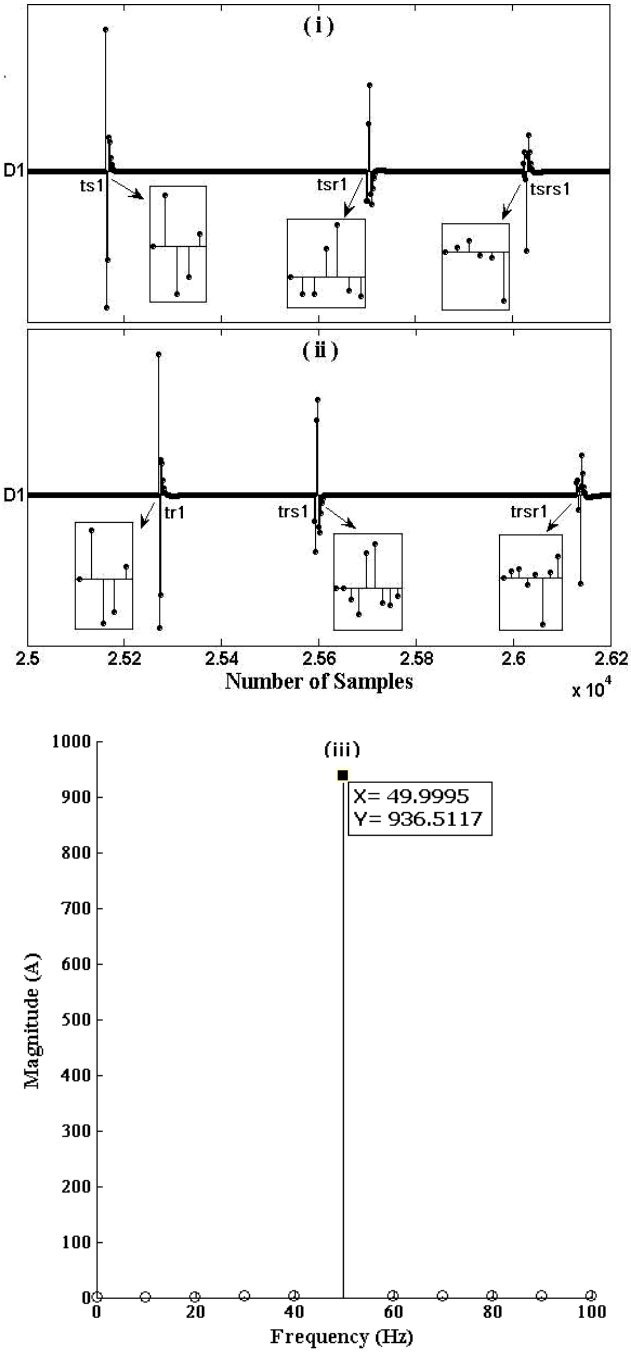

Fig. 10(a): LS fault – V_0 case.

From the FFT analysis, it has been found that LS has rich harmonic contents with the magnitude of the first harmonic of about 940 A for both study cases.

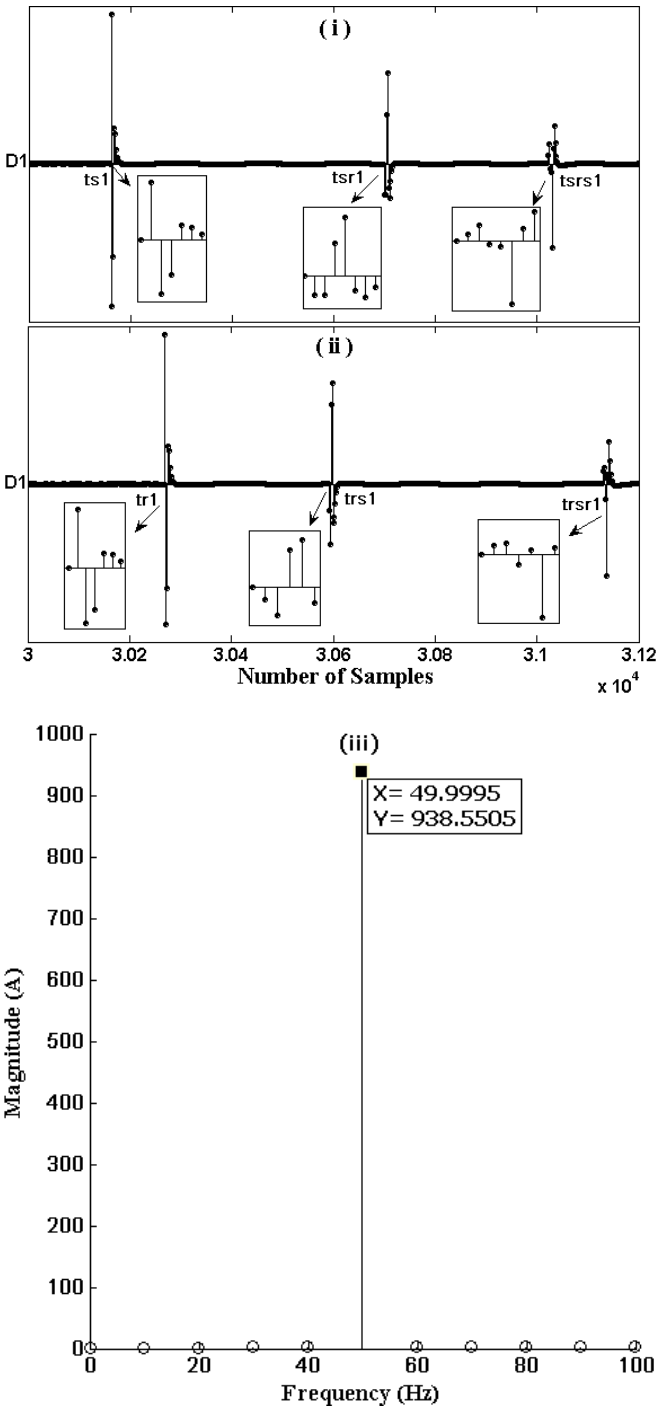

Fig. 10(b): LS fault – V_p case.

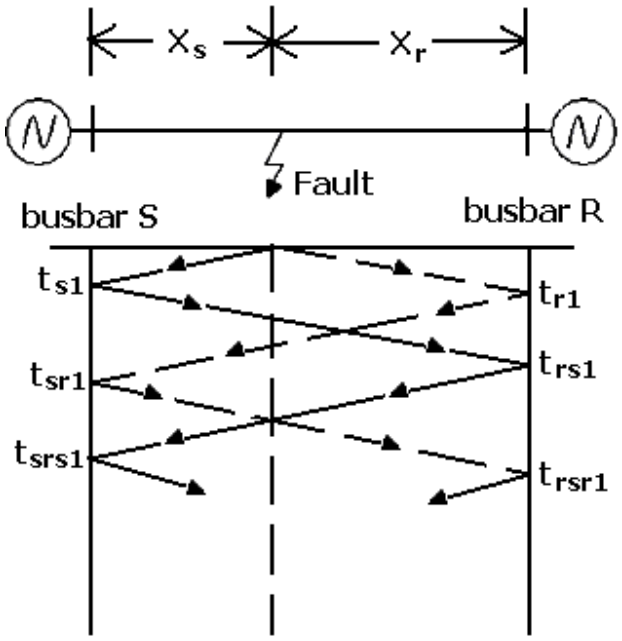

Fig. 11: Lattice diagram for LS case study

Results of TW reflection pattern/ characteristics for four kinds of disturbances, namely SC, OC, HIF and LS have been summarized and given in Table 2.

Table 2
TW reflection patterns for SC, OC, HIF and LS obtained using wavelet transformation on distributed constant parameter Clarke line model

Type of disturbance	Polarities of Wavelet Coefficients		
	S	FP	R
SC	-	-	-
	corrected with Δt= 100 ns		
HIF	-	-	-
OC	-	+	-
LS	-	N/A	-

5 DISCUSSION AND CONCLUSION

This paper has shown that by using the combination of travelling wave characteristic and the harmonic behaviour, it is possible to categorize and classify the type of disturbance occurred on the overhead transmission line. The numerical simulations indicated that in the case of SC faults, waves are inverted at both busbars, and the fault point associated with the highest magnitude of the fundamental component. Spectral analysis shows that among all the study cases, OC has

the smallest magnitude for the first harmonic component while the first harmonic component for HIF lies in between the values for SC and OC cases. For the LS case, WT result shows that it is still possible to locate where the disturbance has occurred even though the LS is not persisting. For the purpose of comparison, parameters such as the time of fault, the line constants, the type of switch or circuit breaker used, etc. are to be taken into consideration while doing the analysis. The result reported is a preliminary investigation to identify the type of faults based on the traveling wave observed at the sending end using distributed constant parameter Clarke line model under perfect conducting ground condition. This study can be further extended to develop intelligent techniques to classify the type of disturbance in a power system. Study on the line-to-line fault and/ or other types of disturbances associated with different kinds of overhead transmission line models are under progress and will be reported shortly.

ACKNOWLEDGEMENTS
Authors would like to thank the Swedish Institute for the sponsorship of the Guest Scholarship Programme with the sponsorship number of 00287/7007-210.

References:
[1] E. E. Ngu, K. Ramar, R. Montano, V. Cooray, A Study on Different Fault Characteristics Using Wavelet and Fast Fourier Transforms, *Proceeding 7th International WSEAS Conference on Application of Electrical Engineering*, 2008, pp. 124-130.
[2] A.R. Almeida, A.K. Barros, M.G. DeSousa, Faults Location in High Voltage Transmission System Using ICA. *International IEEE Conference on Electrical Engineering,* 2007, pp. 1-6.
[3] Z. Q. Bo, A. T. Johns & A. K. Aggarwal, A Novel Fault Locator Based on the Detection of Fault Generated High Frequency Transients, *Proceeding 6th International IEE Conference on Developments in Power Systems Protection,* 1997, pp. 197-200.
[4] D. J. Zhang, Q. H. Wu, Z. Q. Bo & B. Caunce, Transient Position Protection of Lines Using Complex Wavelets Analysis, *IEEE Transaction on Power Delivery,* Vol.18, No.3, 2003, pp. 705-710.
[5] H. Hizam, P. A. Crossley, P. F. Gale & G. Bryson, Fault Section Identification and Location on A Distribution Feeder Using Travelling Waves, *IEEE Power Engineering Society Summer Meeting*, 2002, pp. 1107-1112.
[6] D. Naidoo & N. M. Ijumba, Protection Method for Long HVDC Transmission Lines, *Proceeding 14th International Symposium on High Voltage Engineering,* 2005, pp. 1-6.
[7] C. Y. Evrenosoglu & A. Abur, Traveling Wave Based Fault Location for Teed Circuits, *IEEE Transaction on Power Delivery*, Vol.20, No.2, 2005, pp. 1115-1121.
[8] S. A. Probert & Y. H. Song, Detection and Classification of High Frequency Transients Using Wavelet Analysis, *Proceeding IEEE Power Engineering Society Summer Meeting*, 2002, pp. 801-806.
[9] D. C. Robertson, O. I. Camps, J. S. Mayer & W. B. Gish, Wavelet and Electromagnetic Power System Transients, *IEEE Transaction on Power Delivery,* Vol.11, No.2, 1996, pp. 1050-1056.
[10] S. G. Mallat, A Theory for Multiresolution Signal Decomposition: The Wavelet Representation, *IEEE Transaction Pattern Anal. Machine Intelligent*, Vol.11, No.7, 1989, pp. 674-693.
[11] X. Wang, Q. Qian, & W. Chen, Analyzing Fault-Induced Transients with Wavelets, *Proceeding IEEE Power Engineering Society Summer Meeting*, 2002, pp. 1090-1093.
[12] T. M. Lai, L. A. Snider, E. Lo, & D. Sutanto, High-Impedance Fault Detection Using Discrete Wavelet Transform and Frequency Range and RMS Conversion, *IEEE Transaction on Power Delivery*, Vol.20, No.1, 2005, pp. 397-407.
[13] Naser Zamanan, Jan K. Sykulski, Modelling Arcing High Impedances Faults in Relation to the Physical Processes in the Electric Arc. *WSEAS Transaction on Power Systems,* Vol.8, No.1, 2006, pp. 1507-1512.
[14] Raimundo Nonato M. Machado, Ubiratan H. Bezerra, Evaldo G. Pelaes, Roberto Celio L. De Oliveira, Maria Emilia De Lima Tostes, Classification of Signals with Voltage Disturbance by Means of Wavelet Transform and Intelligent Computational Techniques, *WSEAS Transaction on Power Systems,* Vol.8, No.1, 2006, pp. 1538-1542.
[15] J. Barros, R. I. Diego, Time-Frequency Analysis of Harmonics in Power Systems using Wavelets. *WSEAS Transaction on Circuits and Systems,* Vol.11, No.1, 2006, pp. 1924-1929.